

Observation of reduced $1/f$ noise in graphene field effect transistors on boron nitride substrates

Morteza Kayyalha and Yong P. Chen

Citation: *Applied Physics Letters* **107**, 113101 (2015); doi: 10.1063/1.4930992

View online: <http://dx.doi.org/10.1063/1.4930992>

View Table of Contents: <http://scitation.aip.org/content/aip/journal/apl/107/11?ver=pdfcov>

Published by the AIP Publishing

Articles you may be interested in

[Flicker noise in n-channel nanoscale tri-gate fin-shaped field-effect transistors](#)

Appl. Phys. Lett. **101**, 243512 (2012); 10.1063/1.4772590

[Barrier height dependence of Fano factor and \$1/f\$ noise effect on InGaP based Schottky barrier diode](#)

J. Appl. Phys. **110**, 033721 (2011); 10.1063/1.3619851

[Model of the \$1/f\$ Noise in GaN/AlGaN Heterojunction Field Effect Transistors](#)

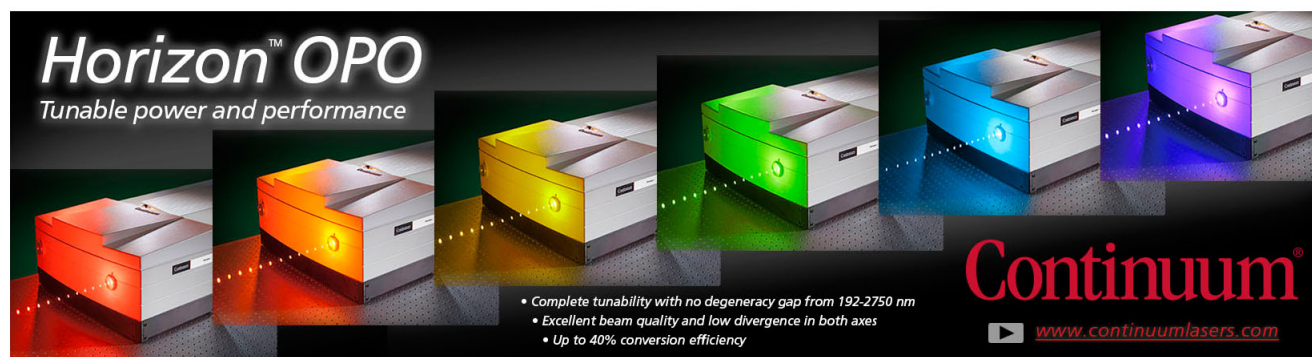
AIP Conf. Proc. **780**, 291 (2005); 10.1063/1.2036752

[Low-frequency noise characteristics of HfSiON gate-dielectric metal-oxide-semiconductor-field-effect transistors](#)

Appl. Phys. Lett. **86**, 082102 (2005); 10.1063/1.1866507

[Evidence for an additional noise source modifying conventional \$1/f\$ frequency dependence in sub- \$\mu\text{m}\$ metal-oxide-semiconductor field-effect transistors](#)

Appl. Phys. Lett. **78**, 380 (2001); 10.1063/1.1339252

The advertisement features a row of five Continuum Horizon OPO laser units, each emitting a different color of light: red, orange, yellow, green, and blue. The units are arranged in a perspective view, with the blue unit on the far right. The background is dark with a grid pattern. The text 'Horizon™ OPO' is prominently displayed in white, with the tagline 'Tunable power and performance' below it. The Continuum logo is in red at the bottom right, with the website 'www.continuumlasers.com' and a play button icon. A list of features is provided in the bottom center.

Horizon™ OPO
Tunable power and performance

- Complete tunability with no degeneracy gap from 192-2750 nm
- Excellent beam quality and low divergence in both axes
- Up to 40% conversion efficiency

Continuum®
www.continuumlasers.com

Observation of reduced 1/f noise in graphene field effect transistors on boron nitride substrates

Morteza Kayyalha^{1,2} and Yong P. Chen^{1,2,3,a)}

¹Birck Nanotechnology Center, Purdue University, West Lafayette, Indiana 47907, USA

²School of Electrical and Computer Engineering, Purdue University, West Lafayette, Indiana 47907, USA

³Department of Physics and Astronomy, Purdue University, West Lafayette, Indiana 47907, USA

(Received 10 August 2015; accepted 2 September 2015; published online 15 September 2015)

We have investigated the low frequency (f) flicker (also called $1/f$) noise of single-layer graphene devices on h-BN (placed on SiO_2/Si) along with those on SiO_2/Si . We observe that the devices fabricated on h-BN have on average one order of magnitude lower noise amplitude compared with devices fabricated on SiO_2/Si despite having comparable mobilities at room temperature. We associate this noise reduction to the lower densities of impurities and trap sites in h-BN than in SiO_2 . Furthermore, the gate voltage dependent noise amplitude shows a broad maximum at Dirac point for devices on h-BN, in contrast to the M-shaped behavior showing a minimum at Dirac point for devices on SiO_2 , consistent with the reduced charge inhomogeneity (puddles) for graphene on h-BN. This study demonstrates that the use of h-BN as a substrate or dielectric can be a simple and efficient noise reduction technique valuable for electronic applications of graphene and other nanomaterials. © 2015 AIP Publishing LLC. [<http://dx.doi.org/10.1063/1.4930992>]

Due to its excellent transport properties and potential in future nano-electronics, graphene has attracted a lot of attention over the past decade.^{1–5} However, lack of sufficient energy gap in graphene limits its applications in digital transistors and electronics. On the other hand, it is shown that graphene may be highly promising for applications in analogue electronics, radio frequency (RF) devices, and sensors where high mobility, gate tunability, and sensitivity to external stimuli are of paramount importance.^{3,6–8} In these applications, low frequency flicker noise also plays a significant role in the performance of the nanoscale devices; particularly because the noise amplitude generally increases as device dimensions shrink.^{9–17}

Several experimental studies have investigated the flicker or $1/f$ noise performance of single-layer or multi-layer graphene devices fabricated on SiO_2 substrates^{9–16,18–20} and on SiC substrates.^{17,21} It is generally believed that flicker noise originates from the fluctuations in the number of charge carriers in the channel due to trapping/detrapping of carriers in the oxide layer and/or fluctuations in the mobility of carriers.^{9,22,23} Also, it has been shown that the carrier mobility in graphene can be highly sensitive to the substrate material, with significant enhancement in mobility at low temperatures when SiO_2 is replaced with h-BN.^{24–26} Therefore, a study of low frequency noise in graphene transistors with h-BN as the substrate is desired for a more complete understanding of the device performance of graphene on h-BN. Such a study is also of interests for the nano-electronics community, where different techniques are actively being explored to reduce the low frequency noise of new materials and devices.

In this work, we investigate the low frequency noise performance of single-layer graphene field effect transistors on h-BN substrates and compare it to those on SiO_2 substrates

(standard doped Si wafer with 300 nm SiO_2), at otherwise similar conditions. Even though the measured *room temperature* mobility does not show significant differences between devices on h-BN and SiO_2 substrates, the normalized noise amplitude is on average one order of magnitude lower for devices on h-BN substrates. We believe that this reduction in the $1/f$ noise amplitude is due to the fact that h-BN has less charge impurities and trapping sites compared to SiO_2 ²⁷ that may help reduce the fluctuations in both mobility and the numbers of carriers in the channel.

We prepare h-BN flakes (with thickness ranging from 20 to 50 nm) using the standard scotch tape exfoliation technique^{2,24,28,29} from commercial h-BN (Momentive Performance Materials Inc.). We then transfer the h-BN flakes onto a substrate of 300 nm-thick SiO_2 on highly doped Si substrate (Nova Electronic Materials). The doped Si will be used as the back gate for our devices. Single-layer graphene flakes are exfoliated also using the scotch tap technique from high quality polycrystalline graphite (Momentive Performance Materials Inc.) onto a polymer film consisting of a thin layer of positive resist (polymethyl methacrylate, PMMA) on top of a thin layer of polyvinyl alcohol (PVA). Using a homemade transfer stage, the graphene flakes are then transferred either on top of SiO_2 or h-BN substrates. The single layer thickness of graphene is confirmed by its characteristic optical contrast and Raman spectrum (measured by a Horiba XploRA Raman microscope with 532 nm excitation laser, with an example of such Raman spectrum of single-layer graphene on h-BN shown in Fig. 1(b)).^{30–32} Finally, e-beam lithography is used to design the contact patterns, followed by deposition of Cr (10 nm) and Au (60 nm) contact electrodes. Figure 1(a) shows an optical image of a representative device on top of an h-BN substrate. We note that no significant change in the noise performance of graphene devices on SiO_2 is observed when graphene is prepared using the standard exfoliation and transfer process^{2,28,29} without the use of PMMA/PVA films.

^{a)}Author to whom correspondence should be addressed. Electronic mail: yongchen@purdue.edu

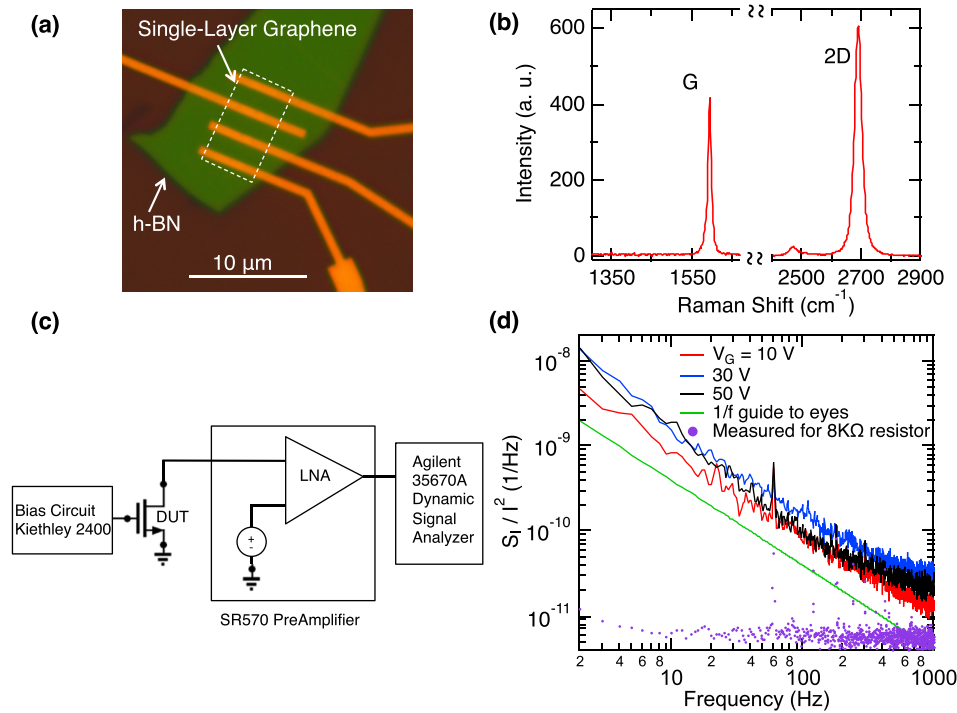


FIG. 1. (a) Optical microscope image of a back-gated field effect transistor based on single-layer graphene on h-BN (on a SiO_2/Si substrate). Scale bar is $10 \mu\text{m}$. (b) Raman spectrum (excitation laser wavelength = 532 nm) of a single-layer graphene measured after transfer on h-BN. The 2D peak at 2680 cm^{-1} has higher intensity than G-peak and has a single-Lorentzian shape with full-width-at-half-maximum (FWHM) $\sim 30 \text{ cm}^{-1}$, indicating a single-layer graphene. The absence of the D peak around 1350 cm^{-1} indicates a low defect density. (c) Schematic of a two-probe noise measurement set-up used in our experiment. A pre-amplifier (SR570) is used to bias the device and also amplifies the current signal (converted to a voltage output) that contains the noise. The spectral density of the current noise is measured with a dynamic signal analyzer. (d) Normalized spectral current noise density (S_I/I^2) of the device shown in (a) as a function of frequency (f) at various back-gate voltages (V_g). Green line (slope = -1 on this log-log plot) is a guide to eyes for the $1/f$ behavior. Background noise is characterized by replacing graphene with an $8 \text{ k}\Omega$ resistor.

All our electrical measurements were performed under ambient conditions (room temperature and atmospheric pressure, and our devices did not go through any thermal annealing processes). A two-probe measurement technique depicted in Figure 1(c) is used for our noise measurements. In this technique, a low noise preamplifier (SR570, input impedance $\sim 1 \Omega$) provides a “silent” (low noise) constant DC voltage bias ($V_{\text{DS}} = 40 \text{ mV}$ for all presented data here unless stated otherwise) across the source and drain of the transistor, and the same amplifier is utilized to amplify the signal (and noise) of the source-drain current (I). The spectral density of the current noise (S_I) is then monitored using a dynamic signal analyzer (Agilent 35670A Dynamic Signal Analyzer). The back-gate voltage (V_g) is supplied by a Keithley 2400 source-meter.

The spectral density (S_I) of the Flicker noise (also known as $1/f$ noise, where f is the frequency) in the current (I) can be expressed as $S_I = \frac{A I^2}{f^\beta}$, where A is the (dimensionless) noise amplitude, and β is the frequency exponent with a value around 1.^{9,22} We observe that the noise spectral density of our devices, regardless of their substrates, is proportional to I^2 (varied by varying V_{DS} at fixed V_g)³³ as previously reported for graphene on SiO_2 .^{9,14,18} Normalized spectral densities of the measured noise signal (S_I/I^2) on a representative graphene device on 40 nm h-BN vs. frequency (f) and at three different V_g 's are plotted in Figure 1(d). As it can be seen, S_I/I^2 is proportional to $1/f^\beta$ with β ranging from 0.85 to 1.2 for our device. We also characterized the background noise by replacing the graphene device with 0.5 , 1 , and $8 \text{ k}\Omega$

resistors (an exemplary result measured for an $8 \text{ k}\Omega$ resistor is also plotted in Figure 1(d)), where the noise amplitude exhibits very weak f dependence and is much smaller than that of our graphene device.

Figure 2(a) shows four-probe resistances (R) of two graphene transistors on SiO_2 and h-BN substrates, respectively, vs. the back-gate voltage ($V_g - V_{\text{D}}$, with respect to the Dirac voltage, V_{D} , which is $\sim 25 \text{ V}$ and $\sim 5 \text{ V}$ for the two devices, respectively). Using the Drude's formula ($\mu_{\text{FE}} = \frac{1}{C_g} \frac{d\sigma}{dV_g}$, where C_g is the gate capacitance per unit area, and σ is the four-probe conductivity of the channel material), we obtain field effect mobility $\mu_{\text{FE}} \sim 4000\text{--}6000 \text{ cm}^2/\text{Vs}$ for both devices. Figure 2(b) shows the drain current (I) vs. $V_g - V_{\text{D}}$ of the same devices of Figure 2(a). These measurements are also done at room temperature and immediately before the noise measurements. Measured drain current values here are later used to calculate the normalized noise spectral density (S_I/I^2) as well as the noise amplitude (A).

In order to have a better comparison between the noise behavior of graphene devices on top of different substrates, we calculate the noise amplitude as $A = \frac{1}{n} \sum_{i=1}^n \frac{f_i S_{Ii}}{I_i^2}$, which is a noise characteristic independent of the current passing through the transistor and averaged over n different frequencies.^{12,15} The quantity (A) and also the normalized noise amplitude ($A \times W \times L$, where W and L are the width and length of the channel, respectively) will be used as metrics to indicate how much improvement in noise we gain by changing different parameters in our devices (e.g., changing the substrate from SiO_2 to h-BN), with larger A indicating a worse noise performance.

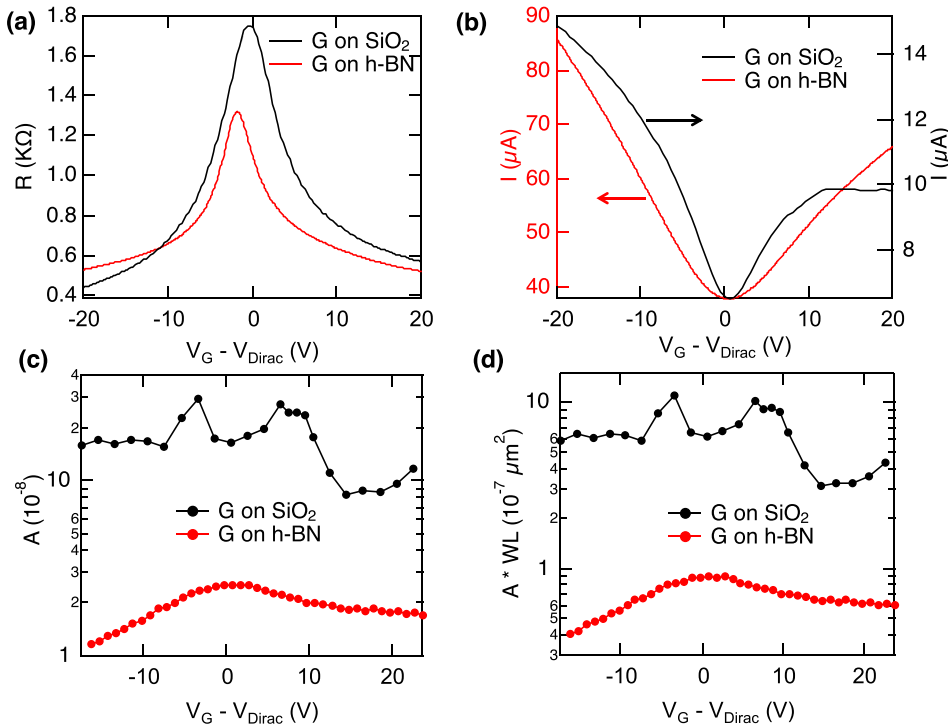


FIG. 2. (a) Four-probe resistance (R) of the graphene channel measured using an AC technique with an SR830 lock-in amplifier vs. $V_g - V_D$ (gate voltage with respect to the Dirac point voltage) for a device on h-BN (red curve) substrate and another on SiO_2 (black curve). (b) DC drain current (I) vs. $V_g - V_D$ of the same devices in (a) measured right before the noise measurements. (c) Amplitude of the noise (A) vs. $V_g - V_D$ and (d) normalized noise amplitude ($A \cdot WL$) vs. $V_g - V_D$ for the devices presented in (a).

Figures 2(c) and 2(d) show the noise amplitude (A) and the normalized noise amplitude ($A \times W \times L$) vs. $V_g - V_D$ in devices studied in Figures 2(a) and 2(b) at room temperature. We notice two significant differences between the graphene device on SiO_2 and that on h-BN. First, the normalized noise amplitude is around one order of magnitude lower in the graphene device on h-BN compared to that on SiO_2 . Previous experiments have demonstrated that h-BN substrate has much lower densities of charge impurities and trap sites compared with SiO_2 and can lead to significantly increased mobility of graphene (particularly at low temperatures, where impurity scattering is especially important for limiting the mobility).^{24,25,34} Since the flicker noise originates from fluctuations in the number or mobility of carriers, the reduced impurities in the h-BN is expected to help reduce these fluctuations and result in lower noise. Second, we observe an M-shaped behavior (with a *minimum* at Dirac point) in the noise amplitude near the Dirac point in the graphene device on SiO_2 , consistent with previous experiments.¹² This behavior is attributed to the existence of electron-hole puddles and charge inhomogeneity near the Dirac point. In contrast, such an M-shaped behavior is not observed for the device on h-BN, where the measured noise amplitude vs. V_g shows a qualitatively similar trend as R vs. V_g and a *maximum* around the Dirac point (where the channel resistance is the largest). The absence of the M-shaped behavior in graphene on h-BN (which we confirmed in multiple devices) is consistent with the expectation that the h-BN substrate can substantially reduce the charge inhomogeneity and electron hole puddles in graphene.^{24,35} The observed gate-dependence of the noise amplitude in graphene devices on h-BN is qualitatively consistent with Hooge's empirical relation ($A = \alpha_H/N$, where N is the total number of carriers, which is tuned by the gate, and α_H is the Hooge's noise parameter).^{9,33}

Figure 3 plots a histogram of the normalized noise amplitudes measured at all the gate voltages for all graphene

devices studied, both on h-BN (data in blue, from 6 devices) and SiO_2 (data in red, from 3 devices; we also included 3 devices from a previous study,¹² shown as data in black). We observe that the noise amplitude of graphene devices is reduced on average by one order of magnitude with h-BN substrate vs. SiO_2 substrate.

A very recent study has shown that encapsulating graphene by h-BN flakes helps reduce noise by 5–10 times while also improves the mobility of the graphene.³⁶ In our work, we also found that the devices on h-BN compared to SiO_2 show on average 10 times improvement in $1/f$ noise, even when similar mobility is observed for devices on both substrates (the absence of notable mobility enhancement in

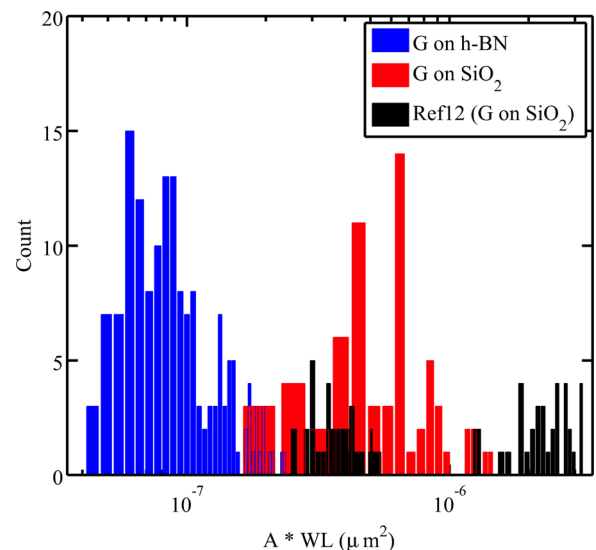


FIG. 3. Histogram of the normalized noise amplitude ($A \cdot WL$) at all the gate voltages measured in all graphene transistors on h-BN (blue, including 6 devices) and on SiO_2 (red, including 3 devices and black, including 3 devices of Ref. 12) substrates.

our devices on h-BN may result from impurities adsorbed on graphene since we did not perform thermal annealing²⁴ nor use the h-BN cap layer³⁶). This suggests that the 1/f noise and mobility in our devices are likely controlled by different aspects of disorder (see also Ref. 15). Our work also suggests one can achieve significantly lower noise by just using h-BN as the substrate without a h-BN cap layer and other more elaborate processing³⁶ involved in fabricating the encapsulated structure.

We have measured the current noise spectral density of graphene field effect transistors on two different substrates, h-BN and SiO₂. We have observed that the normalized noise amplitude of graphene transistors measured at room temperature is reduced by ~10 times for devices on h-BN compared to devices on SiO₂. Furthermore, the gate voltage dependence of the noise amplitude exhibits qualitatively different behaviors for devices on h-BN (with a noise amplitude maximum at Dirac point) versus those on SiO₂ (with a noise amplitude minimum at Dirac point and an M-shaped gate dependence). Our observations can be attributed to the significantly reduced charge impurities and traps in h-BN compared to SiO₂, leading to significantly reduced fluctuations in the carrier mobility and density (including charge puddles) in graphene. Our work demonstrates that the use of h-BN substrates can offer an efficient technique to reduce the noise and improve the performance for graphene-based electronic devices. This approach may also be extended to electronic devices based on other nanomaterials.

We would like to thank Aida Ebrahimi for helpful discussion and also the school of electrical and computer engineering of Purdue University for support.

¹K. S. Novoselov, A. K. Geim, S. V. Morozov, D. Jiang, M. I. Katsnelson, I. V. Grigorieva, S. V. Dubonos, and A. A. Firsov, "Two-dimensional gas of massless Dirac fermions in graphene," *Nature* **438**, 197–200 (2005).
²Y. Zhang, Y. Tan, H. L. Stormer, and P. Kim, "Experimental observation of the quantum Hall effect and Berry's phase in graphene," *Nature* **438**, 201–204 (2005).
³A. K. Geim and K. S. Novoselov, "The rise of graphene," *Nat. Mater.* **6**, 183–191 (2007).
⁴P. Avouris, Z. Chen, and V. Perebeinos, "Carbon-based electronics," *Nat. Nanotechnol.* **2**, 605–615 (2007).
⁵C. Berger, Z. Song, X. Li, X. Wu, N. Brown, C. Naud, D. Mayou, T. Li, J. Hass, A. N. Marchenkov, E. H. Conrad, P. N. First, and W. A. de Heer, "Electronic confinement and coherence in patterned epitaxial graphene," *Science* **312**(5777), 1191–1196 (2006).
⁶F. Schedin, A. K. Geim, S. V. Morozov, E. W. Hill, P. Blake, M. I. Katsnelson, and K. S. Novoselov, "Detection of individual gas molecules adsorbed on graphene," *Nat. Mater.* **6**(9), 652–655 (2007).
⁷F. Schwierz, "Graphene transistors," *Nat. Nanotechnol.* **5**(7), 487–496 (2010).
⁸T. Palacios, A. Hsu, and H. Wang, "Applications of graphene devices in RF communications," *IEEE Commun. Mag.* **48**(6), 122–128 (2010).
⁹Y.-M. M. Lin and P. Avouris, "Strong suppression of electrical noise in bilayer graphene nanodevices," *Nano Lett.* **8**(8), 2119–2125 (2008).
¹⁰A. N. Pal and A. Ghosh, "Resistance noise in electrically biased bilayer graphene," *Phys. Rev. Lett.* **102**(12), 126805 (2009).
¹¹Q. Shao, G. Liu, D. Teweldebrhan, A. A. Balandin, S. Rumyantsev, M. S. Shur, and D. Yan, "Flicker noise in bilayer graphene transistors," *IEEE Electron Device Lett.* **30**(3), 288–290 (2009).
¹²G. Xu, C. M. Torres, Y. Zhang, F. Liu, E. B. Song, M. Wang, Y. Zhou, C. Zeng, and K. L. Wang, "Effect of spatial charge inhomogeneity on 1/f noise behavior in graphene," *Nano Lett.* **10**(9), 3312–3317 (2010).
¹³Y. Zhang, E. E. Mendez, and X. Du, "Mobility-dependent low-frequency noise in graphene field-effect transistors," *ACS Nano* **5**(10), 8124–8130 (2011).

¹⁴A. A. Balandin, "Low-frequency 1/f noise in graphene devices," *Nat. Nanotechnol.* **8**(8), 549–555 (2013).
¹⁵M. Z. Hossain, S. Rumyantsev, M. S. Shur, and A. A. Balandin, "Reduction of 1/f noise in graphene after electron-beam irradiation," *Appl. Phys. Lett.* **102**(15), 153512 (2013).
¹⁶G. Liu, S. Rumyantsev, M. S. Shur, and A. A. Balandin, "Origin of 1/f noise in graphene multilayers: Surface vs. volume," *Appl. Phys. Lett.* **102**(9), 093111 (2013).
¹⁷J. S. Moon, D. Curtis, D. Zehnder, S. Kim, D. K. Gaskill, G. G. Jernigan, R. L. Myers-Ward, C. R. Eddy, P. M. Campbell, K.-M. Lee, and P. Asbeck, "Low-phase-noise graphene FETs in ambipolar RF applications," *IEEE Electron Device Lett.* **32**(3), 270–272 (2011).
¹⁸G. Liu, W. Stillman, S. Rumyantsev, Q. Shao, M. Shur, and A. A. Balandin, "Low-frequency electronic noise in the double-gate single-layer graphene transistors," *Appl. Phys. Lett.* **95**(3), 033103 (2009).
¹⁹I. Heller, S. Chatoor, J. Männik, M. A. G. Zevenbergen, J. B. Oostinga, A. F. Morpurgo, C. Dekker, and S. G. Lemay, "Charge noise in graphene transistors," *Nano Lett.* **10**(5), 1563–1567 (2010).
²⁰S. A. Imam, S. Sabri, and T. Szkopek, "Low-frequency noise and hysteresis in graphene field-effect transistors on oxide," *Micro Nano Lett.* **5**(1), 37–41 (2010).
²¹B. Grandchamp, S. Frégonèse, C. Majek, C. Hainaut, C. Maneux, N. Meng, H. Happy, and T. Zimmer, "Characterization and modeling of graphene transistor low-frequency noise," *IEEE Trans. Electron Devices* **59**(2), 516–519 (2012).
²²A. A. Balandin, *Noise and Fluctuation Control in Electronic Devices* (American Scientific Publishers, Los Angeles, 2002).
²³Y. Lin, J. Appenzeller, J. Knoch, Z. Chen, and P. Avouris, "Low-frequency current fluctuations in individual semiconducting single-wall carbon nanotubes," *Nano Lett.* **6**(5), 930–936 (2006).
²⁴C. R. Dean, A. F. Young, I. Meric, C. Lee, L. Wang, S. Sorgenfrei, K. Watanabe, T. Taniguchi, P. Kim, K. L. Shepard, and J. Hone, "Boron nitride substrates for high-quality graphene electronics," *Nat. Nanotechnol.* **5**, 722–726 (2010).
²⁵A. S. Mayorov, R. V. Gorbachev, S. V. Morozov, L. Britnell, R. Jalil, L. A. Ponomarenko, P. Blake, K. S. Novoselov, K. Watanabe, T. Taniguchi, and A. K. Geim, "Micrometer-scale ballistic transport in encapsulated graphene at room temperature," *Nano Lett.* **11**(6), 2396–2399 (2011).
²⁶A. V. Kretinin, Y. Cao, J. S. Tu, G. L. Yu, R. Jalil, K. S. Novoselov, S. J. Haigh, A. Gholinia, A. Mishchenko, M. Lozada, T. Georgiou, C. R. Woods, F. Withers, P. Blake, G. Eda, A. Wirsig, C. Hucho, K. Watanabe, T. Taniguchi, A. K. Geim, and R. V. Gorbachev, "Electronic properties of graphene encapsulated with different two-dimensional atomic crystals," *Nano Lett.* **14**(6), 3270–3276 (2014).
²⁷W. Gannett, W. Regan, K. Watanabe, T. Taniguchi, M. F. Crommie, and A. Zettl, "Boron nitride substrates for high mobility chemical vapor deposited graphene," *Appl. Phys. Lett.* **98**, 242105 (2011).
²⁸K. S. Novoselov, A. K. Geim, S. V. Morozov, D. Jiang, Y. Zhang, S. V. Dubonos, I. V. Grigorieva, and A. A. Firsov, "Electric field effect in atomically thin carbon films," *Science* **306**, 666–669 (2004).
²⁹K. S. Novoselov, D. Jiang, F. Schedin, T. J. Booth, V. V. Khotkevich, S. V. Morozov, and A. K. Geim, "Two-dimensional atomic crystals," *Proc. Natl. Acad. Sci. U. S. A.* **102**(30), 10451–10453 (2005).
³⁰D. Graf, F. Molitor, K. Ensslin, C. Stampfer, A. Jungen, C. Hierold, and L. Wirtz, "Spatially resolved Raman spectroscopy of single- and few-layer graphene," *Nano Lett.* **7**(2), 238–242 (2007).
³¹A. C. Ferrari and D. M. Basko, "Raman spectroscopy as a versatile tool for studying the properties of graphene," *Nat. Nanotechnol.* **8**(4), 235–246 (2013).
³²A. Eckmann, J. Park, H. Yang, D. Elias, A. S. Mayorov, G. Yu, R. Jalil, K. S. Novoselov, R. V. Gorbachev, M. Lazzeri, A. K. Geim, and C. Casiraghi, "Raman fingerprint of aligned graphene/h-BN superlattices," *Nano Lett.* **13**(11), 5242–5246 (2013).
³³K. K. Hung, P.-K. Ko, C. Hu, and Y. C. Cheng, "A unified model for the flicker noise in metal-oxide-semiconductor field-effect transistors," *IEEE Trans. Electron Devices* **37**(3), 654–665 (1990).
³⁴A. K. Geim and I. V. Grigorieva, "Van der Waals heterostructures," *Nature* **499**(7459), 419–425 (2013).
³⁵J. Xue, J. Sanchez-Yamagishi, D. Bulmash, P. Jacquod, A. Deshpande, K. Watanabe, T. Taniguchi, P. Jarillo-Herrero, and B. J. LeRoy, "Scanning tunnelling microscopy and spectroscopy of ultra-flat graphene on hexagonal boron nitride," *Nat. Mater.* **10**(4), 282–285 (2011).
³⁶M. A. Stolyarov, G. Liu, S. L. Rumyantsev, M. Shur, and A. A. Balandin, "Suppression of 1/f noise in near-ballistic h-BN-graphene-h-BN heterostructure field-effect transistors," *Appl. Phys. Lett.* **107**(2), 023106 (2015).